Available online at www.sciencedirect.com
SCIENCE DIRECT®
International Journal of Heat and Mass Transfer 47 (2004) 4195–4203
International Journal of HEAT and MASS TRANSFER
www.elsevier.com/locate/ijhmt

Radiative heat transfer in discretely heated irregular geometry with an absorbing, emitting, and anisotropically scattering medium using combined Monte-Carlo and finite volume method

Doyoung Byun [a,*], Changjin Lee [a], Seung Wook Baek [b]

[a] Department of Aerospace Engineering, Center of Aerospace System Integration Technology, Konkuk University, 1 Hwayang-Dong, Kwangjin-Gu, Seoul 143-701, Republic of Korea

[b] Division of Aerospace Engineering, Department of Mechanical Engineering, Korea Advanced Institute of Science and Technology, 373-1 Kusong-Dong, Yusung-Gu, Taejon 305-701, Korea

Received 15 March 2004; received in revised form 6 May 2004

Abstract

The ray effects of the finite volume method (FVM) or discrete ordinates method (DOM) are known to show the non-physical oscillations usually observed in the solution of radiative heat transfer on a boundary. This wiggling behavior is caused by the finite discretization of the continuous control angle. This article proposes a combined procedure of the Monte-Carlo and finite-volume method (CMCFVM) for solving radiative heat transfer in absorbing, emitting, and anisotropically scattering medium to eliminate the wiggling behavior. To tackle the ray effect problem, which is especially pronounced in a medium with an isolated boundary heat source, the CMCFVM is suggested here and successfully applied to a two-dimensional irregular geometry.

1. Introduction

In recent years, a study of radiative heat transfer in an irregular multidimensional geometry has received increasing attention with a successive development of more powerful computers. Its practical application resides in a need to accurately predict the thermal behavior in heat exchanger and combustor. Therefore, several methods have been developed to solve the radiative transfer equation in the irregular geometry. Among others, there is the finite volume method (FVM) for radiation [1,2] which has been successfully applied to several problems of body-fitted geometries [3]. Since the spatial domain is divided into a finite number of control volumes in the FVM, this method has a computational compatibility with other control-volume based CFD approach.

The flux methods such as FVM and discrete ordinates method (DOM) used to show a non-physical oscillation in a solution on the boundary heat flux, which results from the ray effect [4,5]. This wiggling behavior is caused by the finite discretization of the continuous control angle. A more detail about this shortcoming in DOM is well described and some remedies are also suggested by Chai et al. [4]. Byun et al. [5] presented that the ray effect is found to be more conspicuous when the heat source is locally isolated in the rather cold medium. To avoid this problem, many researchers have attempted to improve an angular quadrature set as well as a spatial differencing scheme [4,6]. However, most approaches, so far, could not totally correct the ray effects as far as the angular discretization is used over the entire domain. Therefore,

* Corresponding author. Tel.: +82-2-450-4195; fax: +82-2-444-6614.
E-mail address: dybyun@konkuk.ac.kr (D. Byun).

0017-9310/$ - see front matter © 2004 Elsevier Ltd. All rights reserved.
doi:10.1016/j.ijheatmasstransfer.2004.05.008

Nomenclature

I	radiation intensity, W/(m^2 sr)
I_b	blackbody radiation intensity, W/(m^2 sr)
n	number of energy particles absorbed by control volume
$\vec{n}_i$	unit normal vector at the control volume surface i,
N	total number of energy particles emitted
q^R	radiative heat flux, W/m^2
$\vec{r}$	position vector
R	random number
Q	radiative energy
$\vec{s}$	unit direction vector
Greek symbols	
β_0	extinction coefficient, $\kappa_a + \sigma_s$, m^{-1}
θ	polar angle
κ_a	absorption coefficient, m^{-1}
σ	Stefan–Boltzmann constant
σ_s	scattering coefficient, m^{-1}
ϕ	azimuthal angle
Φ	scattering phase function, sr^{-1}
Ψ	scattering angle
ε_w	wall emissivity
ω	single scattering albedo, $= \sigma_s/\beta_0$
Ω	solid angle, sr
$\Delta\Omega$	control angle
Subscript	
w	wall
Superscripts	
m, m'	radiation direction

another alternative for the conventional methods is in high demand to accurately predict the radiative heat transfer.

Ramankutty and Crosbie [7] presented a modified discrete ordinates method as another alternative by applying a separate semi-analytical treatment for the intensities on the boundary and showed the reduction of the ray effects in a partially heated rectangular geometry. However, this method is not appropriate for an irregular complex geometry or for a problem with scattering medium, since a semi-analytical solution is very difficult to obtain. Even more difficult is it for the analytical integration for an anisotropically scattering medium. If the Monte-Carlo method (MCM) [8,9] is employed to analyze the radiative heat transfer, an exact solution can be obtained within a statistical limit while almost eliminating the ray effect. But this method is based on the ray tracing technique so that it needs an enormously large computational time.

Therefore, Baek et al. [10] suggested a simple numerical method, i.e., combined Monte-Carlo and finite volume method (CMCFVM), for analyzing radiative heat transfer in arbitrary configurations. In their work, the CMCFVM is proposed to deal with the ray effects in absorbing, emitting, and isotropic scattering medium which is surrounded by diffusely reflecting walls. Ray effects can be successfully eliminated with a good computational efficiency in a two-dimensional irregular geometry. But the method above has not yet been applied to an analysis of radiative heat transfer in an anisotropic scattering medium and validated in a view of performance.

In this work, the CMCFVM is proposed to deal with the ray effects in absorbing, emitting, and anisotropically scattering medium which is surrounded by diffusely reflecting walls when an isolated heat source is located on the wall. The paper presents radiative heat flux solutions in irregular geometry using the CMCFVM, the Monte-Carlo method, and the FVM. Also the computational efficiency of the CMCFVM is investigated by comparing the solutions of three methods.

2. Formulations of the combined Monte-Carlo and finite-volume method

The radiation intensity for an absorbing, emitting and scattering gray medium at any position, $\vec{r}$, along a path, $\vec{s}$ is governed by

$$\frac{\mathrm{d}I(\vec{r},\vec{s})}{\mathrm{d}s} = -\beta_0 I(\vec{r},\vec{s}) + \kappa_a I_b(\vec{r}) + \frac{\sigma_s}{4\pi}\int_{\Omega'=4\pi} I(\vec{r},\vec{s}')\,\Phi(\vec{s}'\to\vec{s})\,\mathrm{d}\Omega' \quad (1)$$

where κ_a and σ_s are the absorption and scattering coefficients and $\beta_0 = \kappa_a + \sigma_s$ is the extinction coefficient. $\Phi(\vec{s}'\to\vec{s})$ is the scattering phase function for a radiation from incoming direction $\vec{s}'$ to scattered direction $\vec{s}$. The first term on the RHS in Eq. (1) represents an attenuation of radiation intensity due to absorption and out-scattering, while the last two terms account for an augmentation of intensity due to the gas emission as well as in-scattering. The boundary condition for a diffusely emitting and reflecting wall can be denoted by

$$I(\vec{r}_w,\vec{s}) = \varepsilon_w I_b(\vec{r}_w) + \frac{1-\varepsilon_w}{\pi}\int_{\vec{s}'\cdot\vec{n}_w<0} I(\vec{r}_w,\vec{s}')\,|\vec{s}'\cdot\vec{n}_w|\,\mathrm{d}\Omega' \quad (2)$$

where ε_w is the wall emissivity and subscript w denotes the location of the wall, while $\vec{n}_w$ is the unit normal vector.

To implement CMCFVM, above all, the intensity is divided into two parts, i.e., I^{wall} and I^{med}, following the work by Modest [11]

$$I(\vec{r},\vec{s}) = I^{wall}(\vec{r},\vec{s}) + I^{med}(\vec{r},\vec{s}) \tag{3}$$

While I^{wall} originates from the emission from the enclosure wall, I^{med} is traced back to the radiative source term in the medium.

A substitution of Eq. (3) into Eq. (1) results in two radiative transfer equations for I^{wall} and I^{med}. While I^{wall} is governed by the following equation,

$$\frac{dI^{wall}(\vec{r},\vec{s})}{ds} = -\beta_0 I^{wall}(\vec{r},\vec{s}) + \frac{\sigma_s}{4\pi}\int_{\Omega'=4\pi} I^{wall}(\vec{r},\vec{s}')\,\Phi(\vec{s}'\to\vec{s})\,d\Omega' \tag{4}$$

with following boundary condition,

$$I^{wall}(\vec{r}_w,\vec{s}) = \varepsilon_w I_b(\vec{r}_w) + \frac{1-\varepsilon_w}{\pi}\int_{\vec{s}'\cdot\vec{n}_w<0} I^{wall}(\vec{r}_w,\vec{s}')\,|\vec{s}'\cdot\vec{n}_w|\,d\Omega' \tag{5}$$

The governing equation and boundary condition for I^{med} can be written as,

$$\frac{dI^{med}(\vec{r},\vec{s})}{ds} = -\beta_0 I^{med}(\vec{r},\vec{s}) + \kappa_a I_b(\vec{r}) + \frac{\sigma_s}{4\pi}\int_{\Omega'=4\pi} I^{med}(\vec{r},\vec{s}')\,\Phi(\vec{s}'\to\vec{s})\,d\Omega' \tag{6}$$

$$I^{med}(\vec{r}_w,\vec{s}) = \frac{1-\varepsilon_w}{\pi}\int_{\vec{s}'\cdot\vec{n}_w<0} I^{med}(\vec{r}_w,\vec{s}')\,|\vec{s}'\cdot\vec{n}_w|\,d\Omega' \tag{7}$$

Since the emission from the wall is taken into account in Eq. (5), only a reflection term is considered as represented in Eq. (7).

For the case of modified DOM, Ramankutty and Crosbie [7] divided the RTE into two equations by a different way as follows,

$$\frac{dI^{wall}(\vec{r},\vec{s})}{ds} = -\beta_0 I^{wall}(\vec{r},\vec{s}) \tag{8}$$

$$\frac{dI^{med}(\vec{r},\vec{s})}{ds} = -\beta_0 I^{med}(\vec{r},\vec{s}) + \kappa_a I_b(\vec{r}) + \frac{\sigma_s}{4\pi}\int_{\Omega'=4\pi} (I^{wall}+I^{med})(\vec{r},\vec{s}')\,\Phi(\vec{s}'\to\vec{s})\,d\Omega' \tag{9}$$

Then, an analytic solution of Eq. (8) is obtained and substituted into Eq. (9). But when there exists a scattering term, the analytical solution is not available so that Ramankutty and Crosbie [7] deals with the in-scattering term in Eq. (9) using a semi-analytical treatment and a numerical scheme. But this approach requires a tremendous effort for application to a complex irregular geometry or a problem with special boundary condition. Furthermore, a treatment of the anisotropic scattering term introduces an additionally formidable complication.

In this study, while the radiative transfer equation for I^{wall}, Eq. (4) is solved using the Monte-Carlo method rather than trying to find the analytic solution, the radiative transfer equation for I^{med}, Eq. (6) is solved by FVM. The reason for selecting the Monte-Carlo method in solving Eq. (4) is that it can be successfully applied to obtain the exact solution within statistical limit without incurring ray effect. Moreover this method can be easily extended to a multidimensional complex geometry with anisotropic scattering.

In order to implement FVM, Eq. (6) is integrated over a control volume, ΔV, and a control angle, $\Delta\Omega^m$, as shown in Fig. 1, and thereby, the discretization equation is obtained [3,5]. For simplicity, in the following the notation 'med' will be dropped in Eqs. (6) and (7).

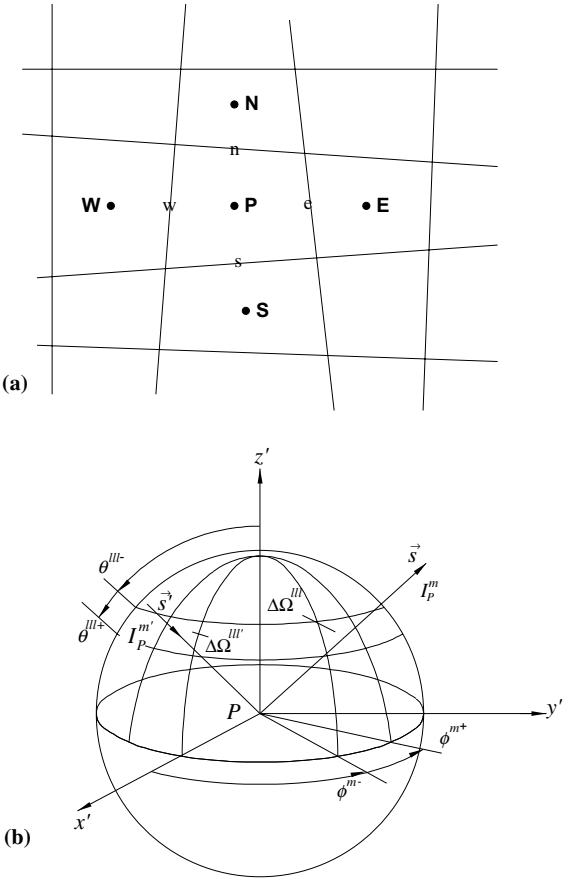

Fig. 1. Schematic of a spatial control volume and control angle.

$$\int_{\Delta\Omega^m}\int_{\Delta A} I^m(\vec{s}\cdot\vec{n}_i)\,\mathrm{d}A\,\mathrm{d}\Omega^m = \int_{\Delta\Omega^m}\int_{\Delta V}(-\beta_0 I^m + S_r^m)\,\mathrm{d}V\,\mathrm{d}\Omega^m \tag{10}$$

$$S_r^m = \kappa_a I_b + \frac{\sigma_s}{4\pi}\int_{\Omega'=4\pi} I^{m'}\Phi^{m'\to m}\,\mathrm{d}\Omega' \tag{11}$$

where superscripts m and m' mean the radiation directions.

By assuming that magnitude of intensity is constant, but its direction varies within control volume and control angle given, following finite-volume formulation can be obtained

$$\sum_{i=e,w,n,s} I_i^m \Delta A_i D_{ci}^m = (-\beta_0 I^m + S_r^m)_P \Delta V\,\Delta\Omega^m \tag{12}$$

where

$$D_{ci}^m = \int_{\Delta\Omega^m}(\vec{s}\cdot\vec{n}_i)\,\mathrm{d}\Omega^m \tag{13}$$

$$\Delta\Omega^m = \int_{m-}^{m+}\mathrm{d}\Omega^m = \int_{\phi^{m-}}^{\phi^{m+}}\int_{\theta^{m-}}^{\theta^{m+}}\sin\theta\,\mathrm{d}\theta\,\mathrm{d}\phi \tag{14}$$

ΔA_i and ΔV represent the surface area and control volume, respectively, while $\vec{n}_i$ is the outward unit normal vector at the control volume face.

Here is adopted a step scheme in which a downstream face intensity is set equal to the upstream nodal value [3]. It is not only simple and convenient, but also ensures positive intensity without considering complex geometric and directional information. By using this scheme, Eq. (12) can be recast into the following general discretization equation, i.e.

$$a_P^m I_P^m = a_E^m I_E^m + a_W^m I_W^m + a_N^m I_N^m + a_S^m I_S^m + b_P^m \tag{15}$$

where

$$a_I^m = \max(-\Delta A_i D_{ci}^m, 0) \tag{16}$$

$$a_P^m = \sum_{i=e,w,n,s}\max(\Delta A_i D_{ci}^m, 0) + \beta_{0,P}\Delta V\Delta\Omega^m \tag{17}$$

$$b_P^m = (S_r^m)_P \Delta V\Delta\Omega^m \tag{18}$$

In Eq. (16), subscript I represents E, W, N, and S while i does e, w, n, and s as shown in Fig. 1, respectively.

Boundary condition in Eq. (7) can be discretized as

$$I_w^m = \frac{1-\varepsilon_w}{\pi}\sum_{D_{cw}^{m'}<0} I_w^{m'}|D_{cw}^{m'}| \tag{19}$$

Using the Monte-Carlo Method, the Eq. (4) for the radiation emitted from the wall is solved by tracing the trajectories of a certain number of particles. Although there are many excellent review papers [12,13], the procedure adopted in the work of Taniguchi et al. [8] is followed here, i.e. radiant energy absorption distribution (READ) method. This method computes the exchange factors involved between elements to determine the radiative heat transfer. Once these factors are obtained for a specific problem, a different set of boundary conditions can be imposed without re-computing the exchange factors. Usually a very large number of bundles is chosen to simulate the radiation emitted from each wall element and then their trajectories are traced to estimate the heat flux or temperature. Because the energy particles are emitted diffusely, a uniform random number is employed, and then the direction of emission of the particle from the wall is as follows,

$$\phi = 2\pi R_\phi \tag{20}$$

$$\theta = \cos^{-1}(1-R_\theta) \tag{21}$$

where θ is polar angle and ϕ azimuthal angle.

Once emitted, an energy particle is absorbed, scattered in the gas medium, or collided with a wall. The penetration distance, along which an energy particle travels before its extinction, is determined by the relation of Beer's law.

$$s = -\ln(1-R_s)/\beta_0 \tag{22}$$

Whether the particle is absorbed or scattered in the gas medium is decided by comparison of a random number and the scattering albedo. Similarly when the particle collides with wall, another random number decides whether the particle is absorbed or reflected using emissivity.

The total radiative energy emitted from wall can be expressed as follows,

$$Q_{out,w} = (1-\alpha)\varepsilon_w\sigma T_w^4\Delta A \tag{23}$$

where α is the self-absorption ratio which represents the ratio of the energy absorbed by the element itself to the total energy emitted from the element. The self-absorption ratio at an arbitrary element I is denoted by

$$\alpha_I = n_I/N_I \tag{24}$$

where the n represents the number of energy absorbed by the element itself, and N the total number of energy emitted by the element. And the amount of the energy emitted from an element I and absorbed by another element J can be expressed using READ, R_{IJ} [8]

$$R_{IJ} = \frac{n_J}{N_I - n_I} \quad (I \neq J) \tag{25}$$

From the Eq. (25), the total amount of the energy absorbed by an element J can be obtained as follows

$$Q_{in,J} = \sum_I R_{IJ} Q_{out,I} \tag{26}$$

The wall heat flux can be evaluated from the net radiative energy

$$q_w^{wall} = (Q_{out,w} - Q_{in,w})/A_w \tag{27}$$

For the combined Monte-Carlo and FVM method, the radiative heat flux at the enclosure wall can be obtained by superimposing each flux component which is calculated from the Monte-Carlo method and FVM, respectively.

$$q_w = q_w^{wall} + q_w^{med} = q_w^{wall} + \int_{\Omega=4\pi} I^{med}(\vec{r}_w, \vec{s})(\vec{s}\cdot\vec{n}_w)\,d\Omega \quad (28)$$

Four Mie-anisotropic scattering phase functions are considered in this study; forward-biased, F1 and F2, and backward-biased, B1 and B2, which are presented by Parthasarathy et al. [9]. F1 and F2 are strongly forward-scattering phase functions, while B1 and B2 are weak back-scattering phase functions. Chu and Churchill [14] expressed the scattering phase function as a series in Legendre polynomials as follows,

$$\Phi(\Psi) = 1 + \sum_{n=1}^{\infty} A_n P_n(\cos\Psi) \quad (29)$$

where Ψ is the scattering angle and A_n is the expansion coefficient. They are obtained by the procedure as suggested by Clark et al. [15] and presented in Table 1.

When the Eq. (6) is solved using the FVM, the Eq. (29) can be substituted into the equation. However to consider anisotropic scattering using the MCM, random numbers have to be generated and then the direction (θ_s, ϕ_s) of scattering of the particle can be decided [9]. For gray medium with scattering phase function, Φ, that is independent of azimuthal angle, the scattering angle, that is identical to polar angle, with respect to the incident direction can be found from

$$R_{\theta s} = \int_0^{\theta_s} \Phi(\theta)\sin\theta\,d\theta \Big/ \int_0^{\pi} \Phi(\theta)\sin\theta\,d\theta \quad (30)$$

The azimuthal angle of scattering is found from

$$\phi_s = 2\pi R_{\phi_s} \quad (31)$$

where R_{θ_s} and R_{ϕ_s} are random numbers between zero and one. θ_s and ϕ_s are the polar and azimuthal angles in the local coordinates with respect to the incident direction.

3. Results and discussions

In order to validate the present codes of Monte-Carlo method and FVM, several preliminary calculations were performed for a two dimensional rectangular geometry as well as the quadrilateral containing an absorbing and emitting medium. The results obtained were found to be in very good agreement with the exact solutions. The present FVM have also been successfully applied to several problems [5,10]. The present Monte-Carlo solutions for isotropic scattering were also validated by comparison with the other solutions [10]. Here, the solutions for anisotropic scattering are validated in a quadrilateral geometry as shown in Fig. 2(a). The emitting surface is taken as the bottom wall, whereas the other walls and the medium are assumed to be cold ($T_w = 0$). All the walls are black and diffuse. The medium is homogeneous and gray with an extinction coefficient of $\beta_0 = 1m^{-1}$. Three different scattering albedos, $\omega = 0.2$, 0.5, and 0.8, are considered with a strong forward-scattering phase function of F1. Fig. 3 shows the radiative heat flux along the top wall normalized by its emitted power. The number of spatial control volumes used for MCM and FVM is $(N_x \times N_y) = (21 \times 21)$. For FVM, the number of control angles is used as $(N_\theta \times N_\phi) = (12 \times 16)$. As shown in the figure, the present solutions are found to be in very good agreement with the other solutions.

Since the Monte-Carlo method requires a large number of energy bundles to produce a sufficiently accurate solution, the number of energy bundles was set to 1×10^7. The variance of the solution in the

Table 1
A_n, the Mie-scattering phase function expansion coefficients

n	F1	F2	B1	B2
0	1.0000000	1.0000000	1.00000	1.00000
1	2.5360217	2.0091653	−0.56524	−1.20000
2	3.5654900	1.5633900	0.29783	0.50000
3	3.9797626	0.6740690	0.08571	
4	4.0029206	0.2221484	0.01003	
5	3.6640084	0.0472529	0.00063	
6	3.0160117	0.0067132		
7	2.2330437	0.0006743		
8	1.3025078	0.0000494		
9	0.5346286			
10	0.2013563			
11	0.0547964			
12	0.0109929			

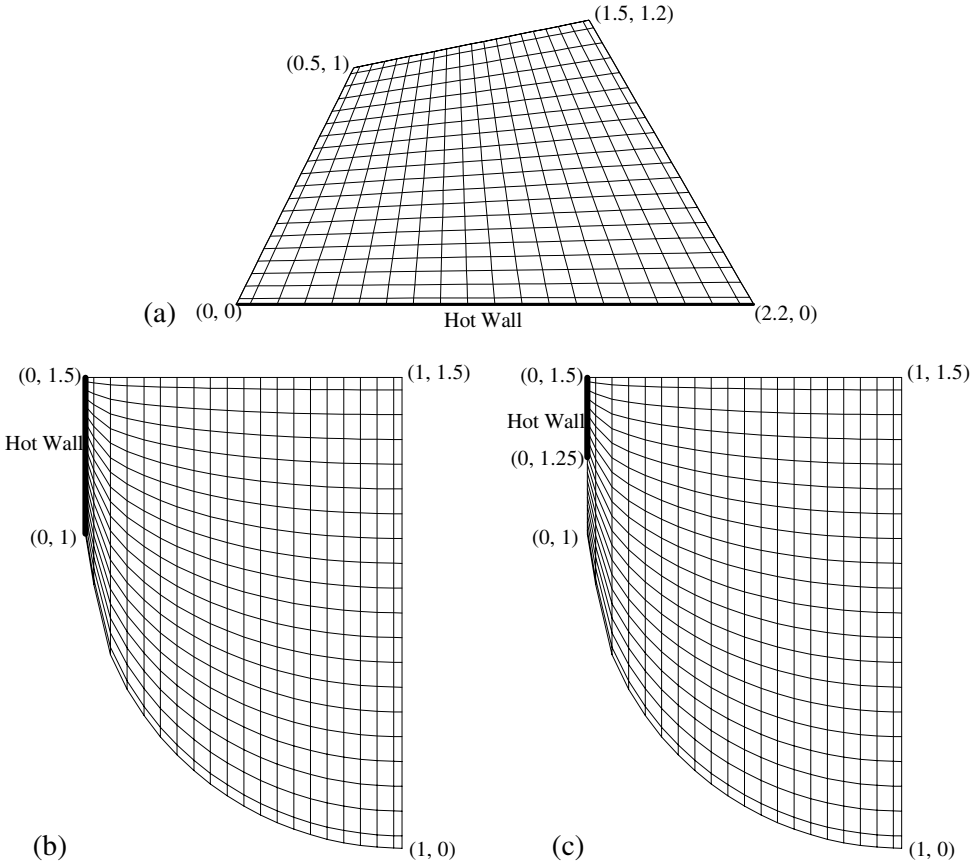

Fig. 2. Schematic of a quadrilateral and curved geometry with a body-fitted coordinate grid system.

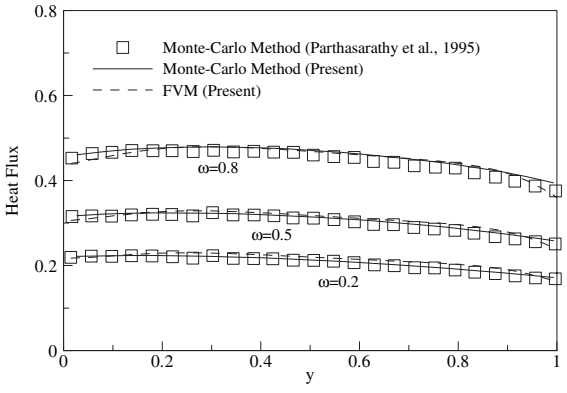

Fig. 3. Comparison of heat fluxes on top wall of a quadrilateral.

Monte-Carlo simulation could be estimated by carrying out several runs with different random number generators. The statistical error for the wall heat flux induced by the Monte-Carlo method was observed to be within 1 percent.

As shown in Fig. 2(b), the combined Monte-Carlo and finite volume method (CMCFVM) is now applied to the curved geometry which is one quarter of a circle with a rectangle on top. The emitting boundary heat source is taken as the straight vertical left wall that is maintained at a constant high temperature of 1000 K. While the left wall is hot, the other walls and medium are cold (300 K). All the walls are assumed to be black and diffuse. The medium is homogeneous and gray with an extinction coefficient of $\beta_0 = 1\ \mathrm{m}^{-1}$. Three different scattering albedos, $\omega = 0.2$, 0.5, and 0.8, are considered with four forward and backward Mie-scattering phase functions as in Table 1. The spatial grid used here is $(N_x \times N_y) = (21 \times 21)$ for CMCFVM and MCM. The numbers of spatial control volumes and control angles used for FVM are $(N_x \times N_y) = (35 \times 35)$ and $(N_\theta \times N_\phi) = (12 \times 16)$, respectively.

Fig. 4(a) and (b) represent the wall heat flux distributions along the right wall of the curved geometry in the absorbing, emitting, and anisotropic scattering medium for F1 and B1 phase functions. The heat flux is non-dimensionalized by the blackbody emissive power of the hot left wall. The results show that the heat flux

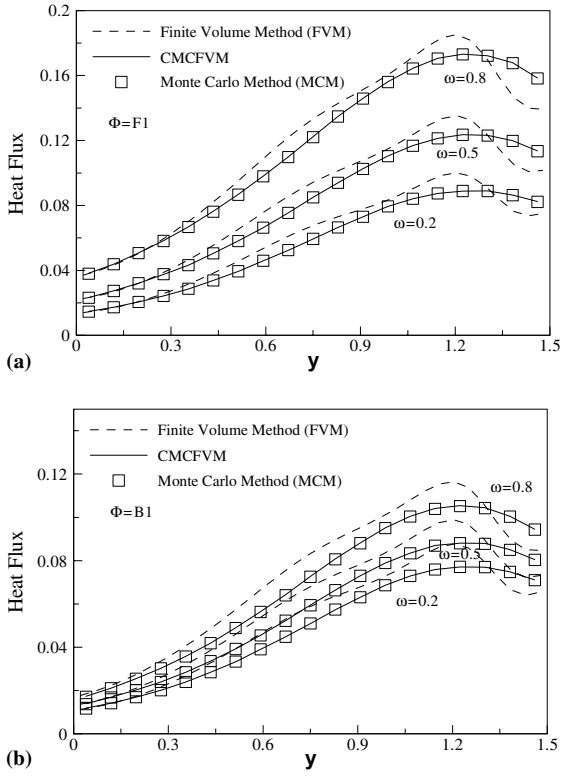

Fig. 4. Effect of scattering albedo on non-dimensional radiative heat flux along the right wall. (a) F1 forward scattering, (b) B1 backward scattering.

increases with scattering albedo for any given phase functions, because the medium absorbs smaller amount of radiative energy as the albedo increases. The forward phase function F1 results in a higher heat flux along the right wall than the backward phase function B1 for three given scattering albedos. In Fig. 4(a) and (b), the solutions by FVM are also compared with those by the Monte-Carlo method. The ray effects are clearly recognized by a wiggling behavior in FVM solution. The ray effects are known to be reduced by simply increasing the number of angular discretization in FVM, but they cannot be totally eliminated for the problem with localized heat source. Therefore, the FVM needs to be corrected to deal with the ray effects. Unlike the results by FVM, the solutions by CMCFVM show a good agreement with those by MCM. The CMCFVM uses the concept of dividing the intensity into two parts which are emitted from isolated heat source and medium, respectively. And then, the wall heat flux is obtained by adding the heat flux obtained by the Monte-Carlo method to that by FVM. It shows a remarkable accuracy achieved by the CMCFVM, which is almost comparable to the Monte-Carlo method with only about 20% of computational time required by the Monte-Carlo method.

In Table 2, the computational time required for F1 forward scattering on a PC equipped with Intel-2GHz CPU and Visual Fortran-5 compiler is listed for comparison. While the CMCFVM requires a longer computation time than FVM which not only lacks in accuracy, but also induces the ray effects, the CMCFVM needs only about 20% of computation time spent by the Monte-Carlo method in generating accurate solutions that are almost comparable to those by MCM. It is also known that the computational time for the finite volume method usually increases as the scattering albedo increases, since more iteration is required to get a convergent solution while resolving the in-scattering as well as out-scattering term. Similarly, the MCM and CMCFVM need more computational time as the scattering albedo becomes larger, since the energy bundles need to travel longer distance to be totally absorbed due to scattering.

Fig. 5 shows the effects of scattering phase functions on the right wall heat fluxes for F1 and F2 forward-scattering phase functions, isotropic scattering, and B1 and B2 backward-scattering phase functions. The heat fluxes for the forward phase functions consistently are shown to be higher than that for isotropic scattering. However, the effects of the backward-scattering phase functions are observed to be relatively smaller than the forward-scattering, based on the case for isotropic scattering case.

Fig. 6 shows the effect of the size of the isolated heat source on the heat flux along the right wall using the Monte-Carlo method, CMCFVM, and FVM. Only an upper half section of the left wall are considered as heat source as shown in Fig. 2(c). All the other conditions such as temperature of the cold medium, extinction coefficient, scattering albedos, and wall boundary

Table 2
Comparison of CPU time for a variety of scattering albedo (F1 case)

ω	CPUs		
	FVM $(N_\theta \times N_\phi) = (18 \times 24)$	CMCFVM $(N_\theta \times N_\phi) = (18 \times 24)$	MCM
0.2	777	3800	15,218
0.5	781	4485	17,854
0.8	808	5386	21,500

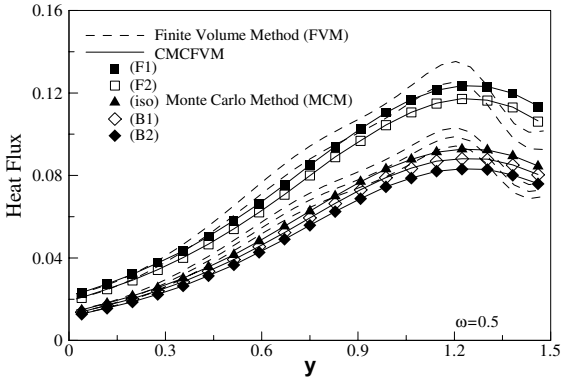

Fig. 5. Effect of scattering phase function on non-dimensional radiative heat flux along the right wall.

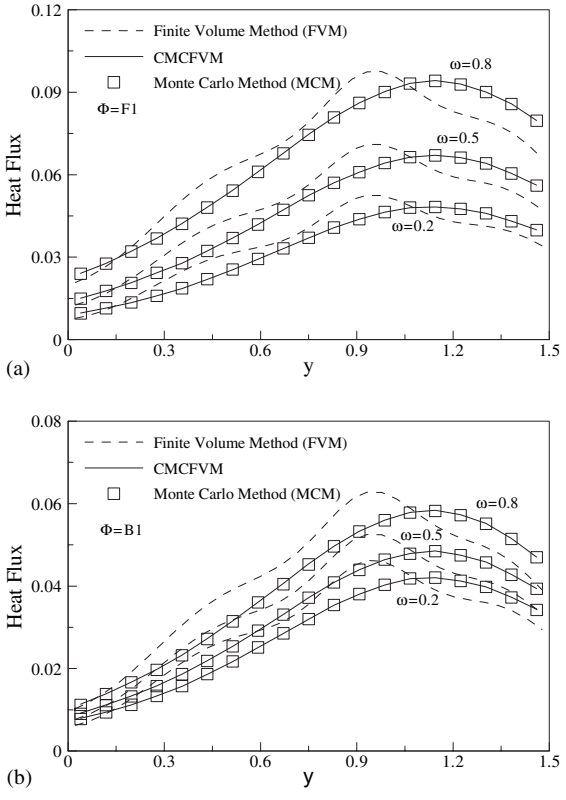

Fig. 6. Effect of scattering albedo on non-dimensional radiative heat flux along the right wall with half size of heat source. (a) F1 forward scattering, (b) B1 backward scattering.

conditions are the same as those for the case in Fig. 4. As the heating size gets smaller, the ray effects are shown to increase when FVM is used. While the results by FVM show a wiggling behavior as well as a significant inaccuracy, the CMCFVM is still observed to produce a very accurate result while still keeping a computational efficiency for both of the forward and backward-scattering phase functions. As the scattering albedo decreases, more radiation is absorbed by the medium so that the wall heat flux gets smaller.

4. Conclusions

In order to examine the ray effects in an absorbing, emitting, and anisotropic scattering medium with an isolated boundary heat source, the radiative heat transfer is analyzed using the combined Monte-Carlo and finite volume method (CMCFVM). And also to discuss its accuracy of the solutions and computational efficiency, the radiative heat fluxes by CMCFVM are compared with the results by the Monte-Carlo method (MCM) and the finite volume method (FVM). Since the CMCFVM makes simultaneously use of the merits of both the Monte-Carlo method and the finite-volume method, it can be easily applied to an irregular complex geometry with a high computational efficiency even when the problem is accompanied by the anisotropic scattering effect.

Acknowledgement

This work was supported by the faculty research fund of Konkuk University in 2003.

References

[1] E.H. Chui, G.D. Raithby, Computation of radiant heat transfer on a nonorthogonal mesh using the finite-volume method, Numer. Heat Transfer Part B 23 (1993) 269–288.
[2] J.C. Chai, H.S. Lee, S.V. Patankar, Finite volume radiative heat transfer procedure for irregular geometries, AIAA J. Thermophys. Heat Transfer 9 (3) (1995) 410–415.
[3] S.W. Baek, M.Y. Kim, J.S. Kim, Nonorthogonal finite-volume solutions of radiative heat transfer in a three-dimensional enclosure, Numer. Heat Transfer Part B 34 (4) (1998) 419–437.
[4] J.C. Chai, H.S. Lee, S.V. Patankar, Ray effect and false scattering in the discrete ordinates method, Numer. Heat Transfer Part B 24 (1993) 359–373.
[5] D.Y. Byun, S.W. Baek, M.Y. Kim, Radiation in discretely heated irregular geometry using Monte-Carlo, finite-volume, and modified discrete-ordinate interpolation method, Numer. Heat Transfer Part A 37 (2000) 1–18.
[6] F. Liu, A. Becker, A. Pollard, Spatial differencing schemes of the discrete-ordinates method, Numer. Heat Transfer Part B 30 (1996) 23–43.
[7] M.A. Ramankutty, A.L. Crosbie, Modified discrete ordinates solution of radiative transfer in two-dimensional rectangular enclosures, J. Quant. Spectrosc. Radiat. Transfer 57 (1) (1997) 107–140.

[8] H. Taniguchi, W.J. Yang, K. Kudo, H. Hayasaka, T. Fukuchi, I. Nakamachi, Monte Carlo method for radiative heat transfer analysis of general gas-particle enclosures, Int. J. Numer. Methods Eng. 25 (1988) 581–592.
[9] G. Parthasarathy, H.S. Lee, J.C. Chai, S.V. Patankar, Monte Carlo solutions for radiative heat transfer in irregular two-dimensional geometries, ASME J. Heat Transfer 117 (1995) 792–794.
[10] S.W. Baek, D.Y. Byun, S.J. Kang, A combined Monte-Carlo and finite-volume method for radiation in a two-dimensional irregular geometry, Int. J. Heat Mass Transfer 43 (2000) 2337–2344.
[11] F.M. Modest, Modified differential approximation for radiative transfer in general three-dimensional media, AIAA J. Thermophys. Heat Transfer 3 (3) (1989) 283–288.
[12] J.P. Howell, Application of Monte Carlo Method to Heat Transfer Problems, in: J.P. Hartnett, T.F. Irvine (Eds.), Advances in Heat Transfer, vol. 5, Academic Press, New York, 1968, pp. 1–54.
[13] A. Haji Sheikh, Monte Carlo Methods, in: W.J. Minkowycz, E.M. Sparrow, R.H. Pletcher, G.E. Schneider (Eds.), Handbook of Numerical Heat Transfer, Wiley, New York, 1988.
[14] C.M. Chu, S.W. Churchill, Representation of the angular distribution of radiation scattered by a spherical particle, J. Opt. Soc. Am. 45 (11) (1955) 958–962.
[15] G.C. Clark, C.M. Chu, S.W. Churchill, Angular distribution coefficients for radiation scattered by a spherical particle, J. Opt. Soc. Am. 47 (1957) 81–84.